SERVICEABILITY

6.1 INTRODUCTION

Chapters 3, 4, and 5 have dealt mainly with the strength design of reinforced concrete beams. Methods have been developed to ensure that beams will have a proper safety margin against failure in flexure or shear, or due to inadequate bond and anchorage of the reinforcement. The member has been assumed to be at a hypothetical overload state for this purpose.

It is also important that member performance in normal service be satisfactory, when loads are those actually expected to act, i.e., when load factors are 1.0. This is not guaranteed simply by providing adequate strength. Service load deflections under full load may be excessively large, or long-term deflections due to sustained loads may cause damage. Tension cracks in beams may be wide enough to be visually disturbing, and in some cases may reduce the durability of the structure. These and other questions, such as vibration or fatigue, require consideration.

Serviceability studies are carried out based on elastic theory, with stresses in both concrete and steel assumed to be proportional to strain. The concrete on the tension side of the neutral axis may be assumed uncracked, partially cracked, or fully cracked, depending on the loads and material strengths (see Section 3.3).

In early reinforced concrete designs, questions of serviceability were dealt with indirectly, by limiting the stresses in concrete and steel at service loads to the rather conservative values that had resulted in satisfactory performance. In contrast, with current design methods that permit more slender members through more accurate assessment of capacity, and with higher-strength materials further contributing to the trend toward smaller member sizes, such indirect methods no longer work. The current approach is to investigate service load cracking and deflections specifically, after proportioning members based on strength requirements.

In this chapter, methods will be developed to ensure that the cracks associated with flexure of reinforced concrete beams are narrow and well distributed, and that short and long-term deflections at loads up to the full service load are not objectionably large.

6.2 CRACKING IN FLEXURAL MEMBERS

All reinforced concrete beams crack, generally starting at loads well below service level, and possibly even prior to loading due to restrained shrinkage. Flexural cracking due to loads is not only inevitable, but actually necessary for the reinforcement to be used effectively. Prior to the formation of flexural cracks, the steel stress is no more

than n times the stress in the adjacent concrete, where n is the modular ratio, E_s/E_c. For materials common in current practice, n is approximately 8. Thus, when the concrete is close to its modulus of rupture of about 500 psi, the steel stress will be only $8 \times 500 = 4000$ psi, far too low to be very effective as reinforcement. At normal service loads, steel stresses 8 or 9 times that value can be expected.

In a well-designed beam, flexural cracks are fine, so-called hairline cracks, almost invisible to the casual observer, and they permit little if any corrosion of the reinforcement. As loads are gradually increased above the cracking load, both the number and width of cracks increase, and at service load level a maximum width of crack of about 0.016 in. is typical. If loads are further increased, crack widths increase further, although the number of cracks is more or less stable.

Cracking of concrete is a random process, highly variable and influenced by many factors. Because of the complexity of the problem, present methods for predicting crack widths are based primarily on test observations. Most equations that have been developed predict the *probable maximum crack width*, which usually means that about 90 percent of the crack widths in the member are below the calculated value. However, isolated cracks exceeding twice the computed width can sometimes occur (Ref. 6.1).

a. Variables Affecting Width of Cracks

In the discussion of the importance of a good bond between steel and concrete in Section 5.1, it was pointed out that if proper end anchorage is provided, a beam will not fail prematurely, even though the bond is destroyed along the entire span. However, crack widths will be greater than for an otherwise identical beam in which good resistance to slip is provided along the length of the span. In general, beams with smooth round bars will display a relatively small number of rather wide cracks in service, while beams with good slip resistance ensured by proper surface deformations on the bars will show a larger number of very fine, almost invisible cracks. Because of this improvement, reinforcing bars in current practice are always provided with surface deformations, the maximum spacing and minimum height of which are established by ASTM Specifications A 615, A 706, and A 996.

A second variable of importance is the stress in the reinforcement. Studies by Gergely and Lutz and others (Refs. 6.2 to 6.4) have confirmed that crack width is proportional to f_s^n, where f_s is the steel stress and n is an exponent that varies in the range from about 1.0 to 1.4. For steel stresses in the range of practical interest, say from 20 to 36 ksi, n may be taken equal to 1.0. The steel stress is easily computed based on elastic cracked-section analysis (Section 3.3b). Alternatively, f_s may be taken equal to $0.60f_y$ according to ACI Code 10.6.4.

Experiments by Broms (Ref. 6.5) and others have shown that both crack spacing and crack width are related to the concrete cover distance d_c, measured from the center of the bar to the face of the concrete. In general, increasing the cover increases the spacing of cracks and also increases crack width. Furthermore, the distribution of the reinforcement in the tension zone of the beam is important. Generally, to control cracking, it is better to use a larger number of smaller-diameter bars to provide the required A_s than to use the minimum number of larger bars, and the bars should be well distributed over the tensile zone of the concrete. For deep flexural members, this includes additional reinforcement on the sides of the web to prevent excessive surface crack widths above the level of the main flexural reinforcement.

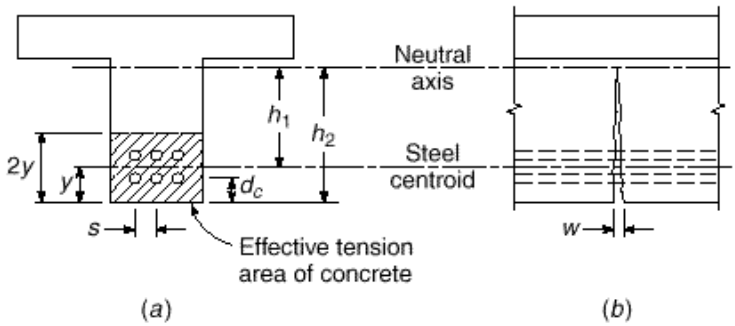

FIGURE 6.1
Geometric basis of crack width calculations.

b. Equations for Crack Width

A number of expressions for maximum crack width have been developed based on the statistical analysis of experimental data. Two expressions that have figured prominently in the development of the crack control provisions in the ACI Code are those developed by Gergely and Lutz (Ref. 6.2) and Frosch (Ref. 6.4) for the maximum crack width at the tension face of a beam. They are, respectively,

$$w = 0.076 \cdot f_s \cdot {}^3\sqrt{d_c A} \tag{6.1}$$

and

$$w = 2000 \frac{f_s}{E_s} \cdot \cdot \sqrt{d_c^2 + \cdot \frac{s}{2} \cdot ^2} \tag{6.2}$$

where w = maximum width of crack, thousandth inches
f_s = steel stress at load for which crack width is to be determined, ksi.
E_s = modulus of elasticity of steel, ksi

The geometric parameters are shown in Fig. 6.1 and are as follows:

d_c = thickness of concrete cover measured from tension face to center of bar closest to that face, in.
$\cdot$ = ratio of distances from tension face and from steel centroid to neutral axis, equal to $h_2 \cdot h_1$
A = concrete area surrounding one bar, equal to total effective tension area of concrete surrounding reinforcement and having same centroid, divided by number of bars, in^2
s = maximum bar spacing, in.

Equations (6.1) and (6.2), which apply only to beams in which deformed bars are used, include all of the factors just named as having an important influence on the width of cracks: steel stress, concrete cover, and the distribution of the reinforcement in the concrete tensile zone. In addition, the factor $\cdot$ is added to account for the increase in crack width with distance from the neutral axis (see Fig. 6.1*b*).

c. Cyclic and Sustained Load Effects

Both cyclic and sustained loading account for increasing crack width. While there is a large amount of scatter in test data, results of fatigue tests and sustained loading tests

indicate that a doubling of crack width can be expected with time (Ref. 6.1). Under most conditions, the spacing of cracks does not change with time at constant levels of sustained stress or cyclic stress range.

6.3 ACI Code Provisions for Crack Control

In view of the random nature of cracking and the wide scatter of crack width measurements, even under laboratory conditions, crack width is controlled in the ACI Code by establishing a maximum center-to-center spacing s for the reinforcement closest to the surface of a tension member as a function of the bar stress under service conditions f_s (in ksi) and the *clear cover* from the nearest surface in tension to the surface of the flexural tension reinforcement c_c.

$$s = \frac{540}{f_s} - 2.5c_c \le 12 \cdot \frac{36}{f_s} \cdot \tag{6.3}$$

The choice of clear cover c_c, rather than the cover to the center of the bar d_c, was made to simplify design, since this allows s to be independent of bar size. As a consequence, maximum crack widths will be somewhat greater for larger bars than for smaller bars.

As shown in Eq. (6.3), the ACI Code sets an upper limit on s of $12(36 \cdot f_s)$. The stress f_s is calculated by dividing the service load moment by the product of the area of reinforcement and the internal moment arm, as shown in Eq. (3.8). Alternatively, the ACI Code permits f_s to be taken as 60 percent of the specified yield strength f_y. For members with only a single bar, s is taken as the width of the extreme tension face.

Figure 6.2*a* compares the values of spacing s obtained using Eqs. (6.1) and (6.2) for a beam containing No. 8 (No. 25) reinforcing bars, for $f_s = 36$ ksi, $\cdot = 1.2$, and a maximum crack width $w = 0.016$ in., to the values calculated using Eq. (6.3). Equations (6.1) and (6.2) give identical spacings for two values of clear cover, but significantly different spacings for other values of c_c. Equation (6.3) provides a practical compromise between the values of s that are calculated using the two experimentally based expressions. The equation is plotted in Fig. 6.2*b* for $f_s = 24$, 36, and 45 ksi, corresponding to $0.60\,f_y$ for Grade 40, 60, and 75 bars, respectively.

ACI Code 10.6.5 points out that the limitation on s in Eq. (6.3) is not sufficient for structures subject to very aggressive exposure or designed to be watertight. In such cases "special investigations or precautions" are required. These include the use of expressions such as Eqs. (6.1) and (6.2) to determine the probable maximum crack width. Further guidance is given in Ref. 6.1.

When concrete T beam flanges are in tension, as in the negative-moment region of continuous T beams, concentration of the reinforcement over the web may result in excessive crack width in the overhanging slab, even though cracks directly over the web are fine and well distributed. To prevent this, the tensile reinforcement should be distributed over the width of the flange, rather than concentrated. However, because of shear lag, the outer bars in such a distribution would be considerably less highly stressed than those directly over the web, producing an uneconomical design. As a reasonable compromise, ACI Code 10.6.6 requires that the tension reinforcement in such cases be distributed over the effective flange width or a width equal to one-tenth the span, whichever is smaller. If the effective flange width exceeds one-tenth the span, some longitudinal reinforcement must be provided in the outer portions of the flange. The amount of such additional reinforcement is left to the discretion of the designer; it

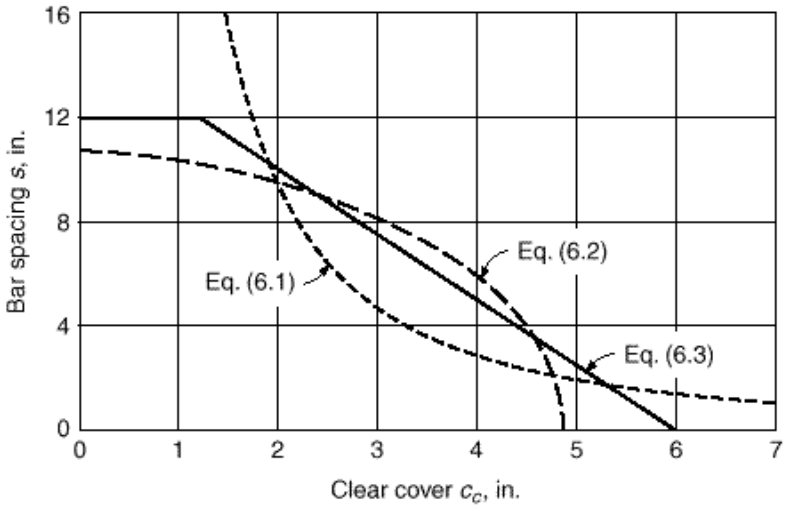

FIGURE 6.2
Maximum bar spacing vs. clear cover: (*a*) Comparison of Eqs. (6.1), (6.2), and (6.3) for w_c = 0.016 in., f_s = 36 ksi, · = 1.2, bar size = No. 8 (No. 25); (*b*) Eq. (6.3) for f_s = 24, 36, and 45 ksi, corresponding to 0.60 f_y for Grade 40, 60, and 75 reinforcement, respectively. (*Part* (*a*) *after Ref. 6.6.*)

should at least be the equivalent of temperature reinforcement for the slab (see Section 13.3), and is often taken as twice that amount.

For beams with relatively deep webs, some reinforcement should be placed near the vertical faces of the web to control the width of cracks in the concrete tension zone above the level of the main reinforcement. Without such steel, crack widths in the web wider than those at the level of the main bars have been observed. According to ACI Code 10.6.7, if the depth of the web exceeds 36 in., longitudinal "skin" reinforcement must be uniformly distributed along both side faces of the member for a distance d· 2 nearest the flexural tension steel. The spacing s_{sk} between longitudinal bars or wires,

each with area A_b, used as skin reinforcement must not exceed the least of $d/2$, 12 in., and $1000\,A_b/(d - 30)$. The *total* area of longitudinal skin reinforcement in both faces need not exceed one-half the area of the required flexural tensile reinforcement. The contribution of the skin steel to flexural strength is usually disregarded, although it may be included in the strength calculations if a strain compatibility analysis is used to establish the stress in the skin steel at the flexural failure load.

Figure 6.2*b* provides a convenient design aid for determining the maximum center-to-center bar spacing as a function of clear cover for the usual case used in design, $f_s = 0.6f_y$. From a practical point of view, it is even more helpful to know the minimum number of bars across the width of a beam stem that is needed to satisfy the ACI Code requirements for crack control. That number depends on side cover, as well as clear cover to the tension face, and is dependent on bar size. Table A.8 in Appendix A gives the minimum number of bars across a beam stem for two common cases, 2 in. clear cover on the sides and bottom, which corresponds to using No. 3 or No. 4 (No. 10 or No. 13) stirrups, and $1\frac{1}{2}$ in. clear cover on the sides and bottom, representing beams in which no stirrups are used.

EXAMPLE 6.1

Check crack control criteria. Figure 6.3 shows the main flexural reinforcement at midspan for a T girder in a high-rise building that carries a service load moment of 7760 in-kips. The clear cover on the side and bottom of the beam stem is $2\frac{1}{4}$ in. Determine if the beam meets the crack control criteria in the ACI Code.

SOLUTION. Since the depth of the web is less than 36 in., skin reinforcement is not needed. To check the bar spacing criteria, the steel stress can be estimated closely by taking the internal lever arm equal to the distance $d - h_f/2$:

$$f_s = \frac{M_s}{A_s/d - h_f/2} = \frac{7760}{7.9 \times 29.25} = 33.6 \text{ ksi}$$

(Alternately, the ACI Code permits using $f_s = 0.60f_y$, giving 36.0 ksi.)

Using f_s in Eq. (6.3) gives

$$s = \frac{540}{f_s} - 2.5c_c = \frac{540}{33.6} - 2.5 \times 2.25 = 10.4 \text{ in.}$$

By inspection, it is clear that this requirement is satisfied for the beam. If the results had been unfavorable, a redesign using a larger number of smaller-diameter bars would have been indicated.

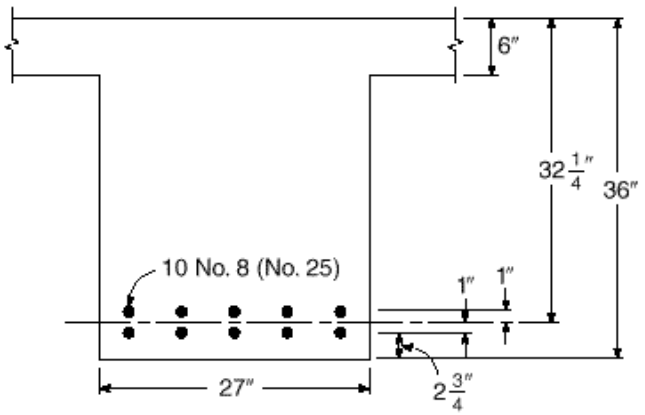

FIGURE 6.3
T beam for crack width determination in Example 6.1.

6.4 CONTROL OF DEFLECTIONS

In addition to limitations on cracking, described in the preceding sections, it is usually necessary to impose certain controls on deflections of beams to ensure serviceability. Excessive deflections can lead to cracking of supported walls and partitions, ill-fitting doors and windows, poor roof drainage, misalignment of sensitive machinery and equipment, or visually offensive sag. It is important, therefore, to maintain control of deflections, in one way or another, so that members designed mainly for strength at prescribed overloads will also perform well in normal service.

There are presently two approaches to deflection control. The first is indirect and consists in setting suitable upper limits on the span-depth ratio. This is simple, and it is satisfactory in many cases where spans, loads and load distributions, and member sizes and proportions fall in the usual ranges. Otherwise, it is essential to calculate deflections and to compare those predicted values with specific limitations that may be imposed by codes or by special requirements.

It will become clear, in the sections that follow, that calculations can, at best, provide a guide to probable actual deflections. This is so because of uncertainties regarding material properties, effects of cracking, and load history for the member under consideration. Extreme precision in the calculations, therefore, is never justified, because highly accurate results are unlikely. However, it is generally sufficient to know, for example, that the deflection under load will be about $\frac{1}{2}$ in. rather than 2 in., while it is relatively unimportant to know whether it will actually be $\frac{5}{8}$ in. rather than $\frac{1}{2}$ in.

The deflections of concern are generally those that occur during the normal service life of the member. In service, a member sustains the full dead load, plus some fraction or all of the specified service live load. Safety provisions of the ACI Code and similar design specifications ensure that, under loads up to the full service load, stresses in both steel and concrete remain within the elastic ranges. Consequently, deflections that occur at once upon application of load, the so-called *immediate deflections*, can be calculated based on the properties either of the uncracked elastic member, the cracked elastic member, or some combination of these (see Section 3.3).

It was pointed out in Sections 2.8 and 2.11, however, that in addition to concrete deformations that occur immediately when load is applied, there are other deformations that take place gradually over an extended period of time. These time-dependent deformations are chiefly due to concrete creep and shrinkage. As a result of these influences, reinforced concrete members continue to deflect with the passage of time. Long-term deflections continue over a period of several years, and may eventually be two or more times the initial elastic deflections. Clearly, methods for predicting both instantaneous and time-dependent deflections are essential.

6.5 IMMEDIATE DEFLECTIONS

Elastic deflections can be expressed in the general form

$$\Delta = \frac{f(\text{loads, spans, supports})}{EI}$$

where EI is the flexural rigidity and f(loads, spans, supports) is a function of the particular load, span, and support arrangement. For instance, the deflection of a uniformly loaded simple beam is $5wl^4/384EI$, so that $f = wl^4/384$. Similar deflection equations

have been tabulated or can easily be computed for many other loadings and span arrangements, simple, fixed, or continuous, and the corresponding f functions can be determined. The particular problem in reinforced concrete structures is therefore the determination of the appropriate flexural rigidity EI for a member consisting of two materials with properties and behavior as widely different as steel and concrete.

If the maximum moment in a flexural member is so small that the tensile stress in the concrete does not exceed the modulus of rupture f_r, no flexural tension cracks will occur. The full, uncracked section is then available for resisting stress and providing rigidity. This stage of loading has been analyzed in Section 3.3a. In agreement with this analysis, the effective moment of inertia for this low range of loads is that of the uncracked transformed section I_{ut}, and E is the modulus of concrete E_c as given by Eq. (2.3). Correspondingly, for this load range,

$$\cdot_{iu} = \frac{f}{E_c I_{ut}} \qquad (a)$$

At higher loads, flexural tension cracks are formed. In addition, if shear stresses exceed v_{cr} [see Eq. (4.3)] and web reinforcement is employed to resist them, diagonal cracks can exist at service loads. In the region of flexural cracks, the position of the neutral axis varies: directly at each crack it is located at the level calculated for the cracked transformed section (see Section 3.3b); midway between cracks it dips to a location closer to that calculated for the uncracked transformed section. Correspondingly, flexural-tension cracking causes the effective moment of inertia to be that of the cracked transformed section in the immediate neighborhood of flexural-tension cracks, and closer to that of the uncracked transformed section midway between cracks, with a gradual transition between these extremes.

It is seen that the value of the local moment of inertia varies in those portions of the beam in which the bending moment exceeds the cracking moment of the section

$$M_{cr} = \frac{f_r I_{ut}}{y_t} \qquad (6.4)$$

where y_t is the distance from the neutral axis to the tension face and f_r is the modulus of rupture. The exact variation of I depends on the shape of the moment diagram and on the crack pattern, and is difficult to determine. This makes an exact deflection calculation impossible.

However, extensively documented studies (Ref. 6.7) have shown that deflections Δ_{ic} occurring in a beam after the maximum moment M_a has reached and exceeded the cracking moment M_{cr} can be calculated by using an effective moment of inertia I_e; that is,

$$\cdot_{ic} = \frac{f}{E_c I_e} \qquad (b)$$

where

$$I_e = \cdot \frac{M_{cr}}{M_a} \cdot^3 I_{ut} + \cdot 1 - \cdot \frac{M_{cr}}{M_a} \cdot^3 \cdot I_{cr} \le I_{ut} \qquad (6.5)$$

and I_{cr} is the moment of inertia of the cracked transformed section.

In Fig. 6.4, the effective moment of inertia, given by Eq. (6.5), is plotted as a function of the ratio $M_a \cdot M_{cr}$ (the reciprocal of the moment ratio used in the equation). It is seen that, for values of maximum moment M_a less than the cracking moment M_{cr},

FIGURE 6.4
Variation of I_e with moment ratio.

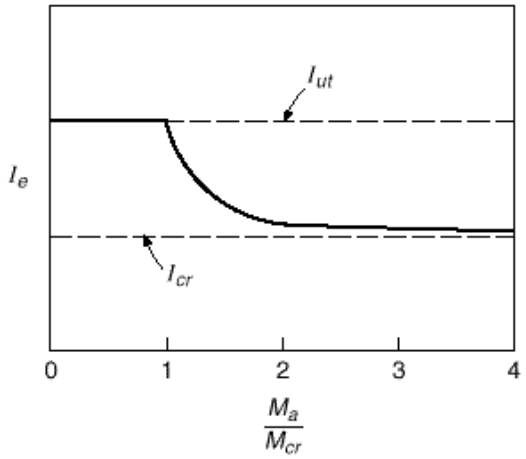

FIGURE 6.5
Deflection of a reinforced concrete beam.

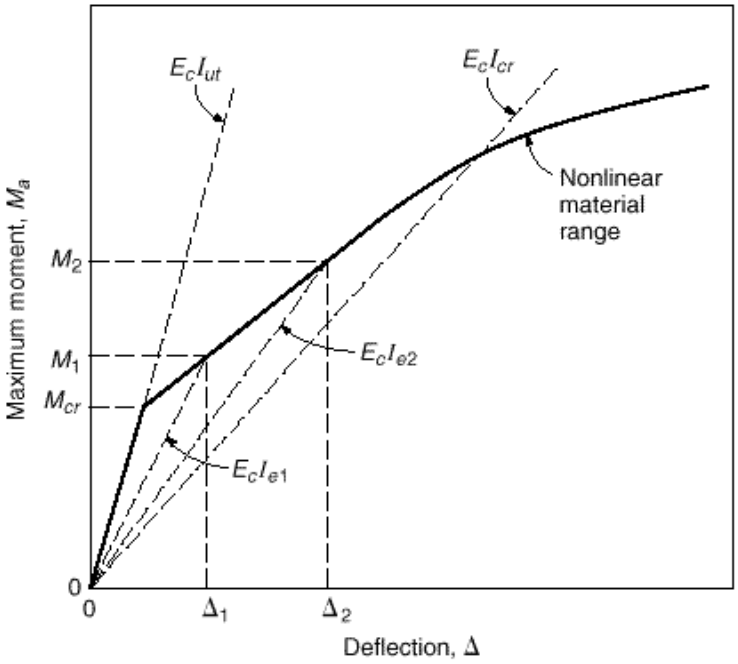

that is, $M_a \cdot M_{cr}$ less than 1.0, $I_e = I_{ut}$. With increasing values of M_a, I_e approaches I_{cr}, and for values of $M_a \cdot M_{cr}$ of 3 or more, I_e is almost the same as I_{cr}. Typical values of $M_a \cdot M_{cr}$ at full service load range from about 1.5 to 3.

Figure 6.5 shows the growth of deflections with increasing moment for a simple-span beam, and illustrates the use of Eq. (6.5). For moments no larger than M_{cr}, deflections are practically proportional to moments and the deflection at which cracking begins is obtained from Eq. (*a*) with $M = M_{cr}$. At larger moments, the effective moment of inertia I_e becomes progressively smaller, according to Eq. (6.5), and deflections are found by Eq. (*b*) for the load level of interest. The moment M_2 might correspond to the full service load, for example, while the moment M_1 would represent the dead load moment for a typical case. A moment-deflection curve corresponding to the line E_cI_{cr}

represents an upper bound for deflections, consistent with Fig. 6.4, except that at loads somewhat beyond the service load, the nonlinear response of steel or concrete or both causes a further nonlinear increase in deflections.

Note that to calculate the increment of deflection due to live load, causing a moment increase $M_2 - M_1$, a two-step computation is required: the first for deflection Δ_2 due to live and dead load, and the second for deflection Δ_1 due to dead load alone, each with the appropriate value of I_e. Then the deflection increment due to live load is found, equal to $\Delta_2 - \Delta_1$.

Most reinforced concrete spans are continuous, not simply supported. The concepts just introduced for simple spans can be applied, but the moment diagram for a given span will include both negative and positive regions, reflecting the rotational restraint provided at the ends of the spans by continuous frame action. The effective moment of inertia for a continuous span can be found by a simple averaging procedure, according to the ACI Code, that will be described in Section 6.7c.

A fundamental problem for continuous spans is that, although the deflections are based on the moment diagram, that moment diagram depends, in turn, on the flexural rigidity *EI* for each member of the frame. The flexural rigidity depends on the extent of cracking, as has been demonstrated. Cracking, in turn, depends on the moments, which are to be found. The circular nature of the problem is evident.

One could use an iterative procedure, initially basing the frame analysis on uncracked concrete members, determining the moments, calculating effective *EI* terms for all members, then recalculating moments, adjusting the *EI* values, etc. The process could be continued for as many iterations as needed, until changes are not significant. However, such an approach would be expensive and time-consuming, even with computer use.

Usually, a very approximate approach is adopted. Member flexural stiffnesses for the frame analysis are based simply on properties of uncracked rectangular concrete cross sections. This can be defended noting that the moments in a continuous frame depend only on the *relative* values of *EI* in its members, not the *absolute* values. Hence, if a consistent assumption, i.e., uncracked section, is used for all members, the results should be valid. Although cracking is certainly more prevalent in beams than in columns, thus reducing the relative *EI* for the beams, this is compensated to a large extent, in typical cases, by the stiffening effect of the flanges in the positive bending regions of continuous T beam construction. This subject is discussed at greater length in Section 12.5.

6.6 Deflections Due to Long-Term Loads

Initial deflections are increased significantly if loads are sustained over a long period of time, due to the effects of shrinkage and creep. These two effects are usually combined in deflection calculations. Creep generally dominates, but for some types of members, shrinkage deflections are large and should be considered separately (see Section 6.8).

It was pointed out in Section 2.8 that creep deformations of concrete are directly proportional to the compressive stress up to and beyond the usual service load range. They increase asymptotically with time and, for the same stress, are larger for low-strength than for high-strength concretes. The ratio of additional time-dependent strain to initial elastic strain is given by the creep coefficient C_{cu} (see Table 2.1).

For a reinforced concrete beam, the long-term deformation is much more complicated than for an axially loaded cylinder, because while the concrete creeps under

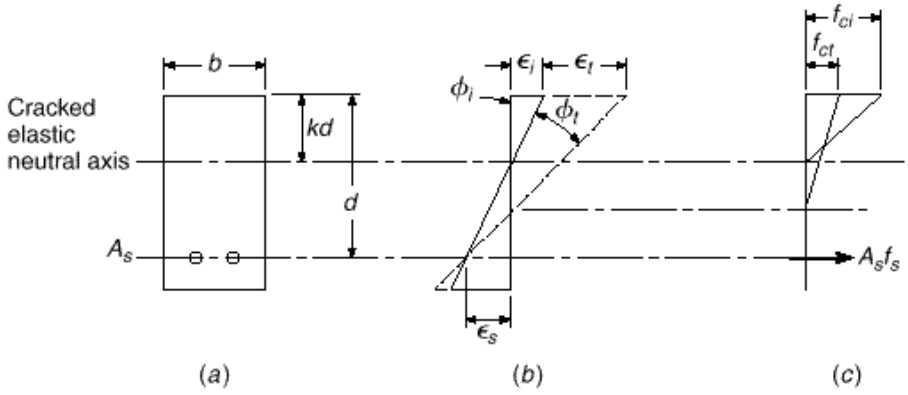

FIGURE 6.6
Effect of concrete creep on curvature: (*a*) beam cross section; (*b*) strains; (*c*) stresses and forces. (*Adapted from Ref. 6.8.*)

sustained load, the steel does not. The situation in a reinforced concrete beam is illustrated by Fig. 6.6. Under sustained load, the initial strain $\cdot_i$ at the top face of the beam increases, due to creep, by the amount $\cdot_t$, while the strain $\cdot_s$ in the steel is essentially unchanged. Because the rotation of the strain distribution diagram is therefore about a point at the level of the steel, rather than about the cracked elastic neutral axis, the neutral axis moves down as a result of creep, and

$$\frac{\cdot_t}{\cdot_i} \cdot \frac{\cdot_t}{\cdot_i} \qquad (a)$$

demonstrating that the usual creep coefficients could not be applied to initial curvatures to obtain creep curvatures (hence deflections).

The situation is further complicated. Due to the lowering of the neutral axis associated with creep (see Fig. 6.6*b*) and the resulting increase in compression area, the compressive stress required to produce a given resultant C to equilibrate $T = A_s f_s$ is less than before, in contrast to the situation in a creep test of a compressed cylinder, because the beam creep occurs at a gradually diminishing stress. On the other hand, with the new lower neutral axis, the internal lever arm between compressive and tensile resultant forces is less, calling for an increase in both resultants for a constant moment. This, in turn, will require a small increase in stress, and hence strain, in the steel; thus, $\cdot_s$ is not constant as assumed originally.

Because of such complexities, it is necessary in practice to calculate additional, time-dependent deflections of beams due to creep (and shrinkage) using a simplified, empirical approach by which the initial elastic deflections are multiplied by a factor $\cdot$ to obtain the additional long-time deflections. Values of $\cdot$ for use in design are based on long-term deflection data for reinforced concrete beams (Refs. 6.8 to 6.11). Thus

$$\cdot_t = \cdot \cdot_i \qquad (6.6)$$

where Δ_t is the *additional* long-term deflection due to the combined effect of creep and shrinkage, and Δ_i is the initial elastic deflection calculated by the methods described in Section 6.5.

The coefficient $\cdot$ depends on the duration of the sustained load. It also depends on whether the beam has only reinforcement A_s on the tension side, or whether additional longitudinal reinforcement A'_s is provided on the compression side. In the latter case, the long-term deflections are much reduced. This is so because when no compression reinforcement is provided, the compression concrete is subject to unrestrained creep and shrinkage. On the other hand, since steel is not subject to creep, if

additional bars are located close to the compression face, they will resist and thereby reduce the amount of creep and shrinkage and the corresponding deflection (Ref. 6.11). Compression steel may be included for this reason alone. Specific values of $\cdot$, used to account for the influence of creep and compression reinforcement, will be given in Section 6.7.

If a beam carries a certain sustained load W (e.g., the dead load plus the average traffic load on a bridge) and is subject to a short-term heavy live load P (e.g., the weight of an unusually heavy vehicle), the maximum total deflection under this combined loading is obtained as follows:

1. Calculate the instantaneous deflection Δ_{iw} caused by the sustained load W by methods given in Section 6.5.
2. Calculate the additional long-term deflection caused by W; i.e.,

$$\cdot_{tw} = \cdot \cdot_{iw}$$

3. Then the total deflection caused by the sustained part of the load is

$$\cdot_{w} = \cdot_{iw} + \cdot_{tw}$$

4. In calculating the additional instantaneous deflection caused by the short-term load P, account must be taken of the fact that the load-deflection relation after cracking is nonlinear, as illustrated by Fig. 6.5. Hence

$$\cdot_{ip} = \cdot_{i(w+p)} - \cdot_{iw}$$

where $\Delta_{i(w+p)}$ is the total instantaneous deflection that would be obtained if W and P were applied simultaneously, calculated by using I_e determined for the moment caused by $W + P$.

5. Then the total deflection under the sustained load plus heavy short-term load is

$$\cdot = \cdot_{w} + \cdot_{ip}$$

In calculations of deflections, careful attention must be paid to the load history, i.e., the time sequence in which loads are applied, as well as to the magnitude of the loads. The short-term peak load on the bridge girder just described might be applied early in the life of the member, before time-dependent deflections had taken place. Similarly, for buildings, heavy loads such as stacked material are often placed during construction. These temporary loads may be equal to, or even greater than, the design live load. The state of cracking will correspond to the *maximum load* that was carried, and the sustained load deflection, on which the long-term effects are based, would correspond to that cracked condition. I_e for the maximum load reached should be used to recalculate the sustained load deflection before calculating long-term effects.

This will be illustrated referring to Fig. 6.7, showing the load-deflection plot for a building girder that is designed to carry a specified dead and live load. Assume first that the dead and live loads increase monotonically. As the full dead load W_d is applied, the load deflection curve follows the path 0-1, and the dead load deflection, Δ_d, is found using I_{e1} calculated from Eq. (6.5), with $M_a = M_d$. The time-dependent effect of the dead load would be $\cdot \Delta_d$. As live load is then applied, path 1-2 would be followed. Live load deflection, Δ_l, would be found in two steps, as described in Section 6.5, first finding Δ_{d+l} based on I_{e2}, with M_a in Eq. (6.5) equal to M_{d+l}, and then subtracting dead load deflection Δ_d.

If, on the other hand, short-term construction loads were applied, then removed, the deflection path 1-2-3 would be followed. Then, under dead load only, the resulting deflection would be $\cdot_{d}$. Note that this deflection can be found in one step using W_d,

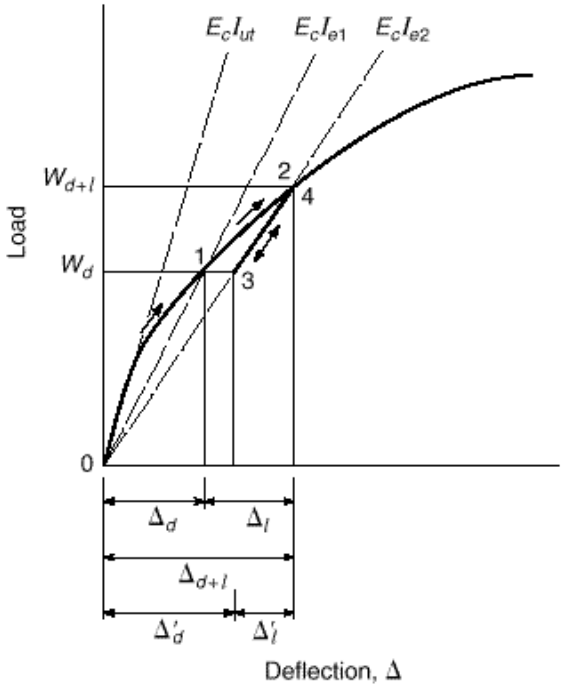

FIGURE 6.7
Effect of load history on deflection of a building girder.

but with I_{e2} corresponding to the maximum load reached. The long-term deflection now would be Δ'_d, significantly *larger* than before. Should the full design *live* load then be applied, the deflection would follow path 3-4, and the live load deflection would be *less* than for the first case. It, too, can be calculated by a simple one-step calculation using W_l alone, in this case, and with moment of inertia equal to I_{e2}.

Clearly, in calculating deflections, the engineer must anticipate, as nearly as possible, both the magnitude and time-sequence of the loadings. Although long-term deflections are often calculated assuming monotonic loading, with both immediate and long-term effects of dead load occurring before application of live load, in many cases this is not realistic.

6.7 ACI Code Provisions for Control of Deflections

a. Minimum Depth-Span Ratios

As pointed out in Section 6.4, two approaches to deflection control are in current use, both acceptable under the provisions of the ACI Code, within prescribed limits. The simpler of these is to impose restrictions on the minimum member depth h, relative to the span l, to ensure that the beam will be sufficiently stiff that deflections are unlikely to cause problems in service. Deflections are greatly influenced by support conditions (e.g., a simply supported uniformly loaded beam will deflect 5 times as much as an otherwise identical beam with fixed supports), so minimum depths must vary depending on conditions of restraint at the ends of the spans.

According to ACI Code 9.5.2, the minimum depths of Table 6.1 apply to one-way construction *not* supporting or attached to partitions or other construction likely to be damaged by large deflections, unless computation of deflections indicates a

TABLE 6.1
Minimum thickness of nonprestressed beams or one-way slabs unless deflections are computed

Member	Minimum Thickness, ·			
	Simply Supported	One End Continuous	Both Ends Continuous	Cantilever
	Members not supporting or attached to partitions or other construction likely to be damaged by large deflections			
Solid one-way slabs	*l*·20	*l*·24	*l*·28	*l*·10
Beams or ribbed one-way slabs	*l*·16	*l*·18.5	*l*·21	*l*·8

lesser depth can be used without adverse effects. Values given in Table 6.1 are to be used directly for normal-weight concrete with $w_c = 145$ pcf and reinforcement with $f_y = 60{,}000$ psi. For members using lightweight concrete with density in the range from 90 to 120 pcf, the values of Table 6.1 should be multiplied by $(1.65 - 0.005w_c) \geq 1.09$. For yield strengths other than 60,000 psi, the values should be multiplied by $(0.4 + f_y \cdot 100{,}000)$.

b. Calculation of Immediate Deflections

When there is need to use member depths shallower than are permitted by Table 6.1, or when members support construction that is likely to be damaged by large deflections, or for prestressed members, deflections must be calculated and compared with limiting values (see Section 6.7e). The calculation of deflections, when required, proceeds along the lines described in Sections 6.5 and 6.6. For design purposes, the moment of the uncracked transformed section I_{ut} can be replaced by that of the gross concrete section I_g, neglecting reinforcement, without serious error. With this simplification, Eqs. (6.4) and (6.5) are replaced by the following:

$$M_{cr} = \frac{f_r I_g}{y_t} \tag{6.7}$$

and

$$I_e = \left(\frac{M_{cr}}{M_a}\right)^3 I_g + \left[1 - \left(\frac{M_{cr}}{M_a}\right)^3\right] I_{cr} \leq I_g \tag{6.8}$$

The modulus of rupture for normal-weight concrete is to be taken equal to

$$f_r = 7.5\lambda\sqrt{f'_c} \tag{6.9a}$$

For lightweight concrete, the modulus of rupture may not be known, but the split-cylinder strength f_{ct} is often specified and determined by tests. For normal-weight concretes, the split-cylinder strength is generally assumed to be $f_{ct} = 6.7\lambda\sqrt{f'_c}$. Accordingly, in Eq. (6.9*a*), $f_{ct}/6.7$ can be substituted for $\lambda\sqrt{f'_c}$ for the purpose of calculating the modulus of rupture. Then for lightweight concrete, if f_{ct} is known,

$$f_r = 7.5\frac{f_{ct}}{6.7} = 1.12f_{ct} \tag{6.9b}$$

where $f_{ct} \cdot 6.7$ is not to exceed $\cdot \overline{f_c}$ according to ACI Code 9.5.2. In lieu of test information on tensile strength, f_r can be calculated by Eq. (6.9*a*) multiplied by 0.75 for "all-lightweight" concrete and 0.85 for "sand-lightweight" concrete.

c. Continuous Spans

For continuous spans, ACI Code 9.5.2 calls for a simple average of values obtained from Eq. (6.8) for the critical positive- and negative-moment sections, i.e.,

$$I_e = 0.50I_{em} + 0.25 \cdot I_{e1} + I_{e2} \cdot \tag{6.10a}$$

where I_{em} is the effective moment of inertia for the midspan section and I_{e1} and I_{e2} those for the negative-moment sections at the respective beam ends, each calculated from Eq. (6.8) using the applicable value of M_a. It is shown in Ref. 6.12 that a somewhat improved result can be had for continuous prismatic members using a weighted average for beams with both ends continuous of

$$I_e = 0.70I_{em} + 0.15 \cdot I_{e1} + I_{e2} \cdot \tag{6.10b}$$

and for beams with one end continuous and the other simply supported of

$$I_e = 0.85I_{em} + 0.15I_{e1} \tag{6.10c}$$

where I_{e1} is the effective moment of inertia at the continuous end. The ACI Code, as an option, also permits use of I_e for continuous prismatic beams to be taken equal to the value obtained from Eq. (6.8) at midspan; for cantilevers, I_e calculated at the support section may be used.

After I_e is found, deflections may be computed using the moment-area method (Ref. 6.13), with due regard for rotations of the tangent to the elastic curve at the supports. In general, in computing the maximum deflection, the loading producing the maximum positive moment may be used, and the midspan deflection may normally be used as an acceptable approximation of the maximum deflection. Coefficients for deflection calculation such as derived by Branson in Ref. 6.7 are helpful. For members where supports may be considered fully fixed or hinged, handbook equations for deflections may be used.

d. Long-Term Deflection Multipliers

On the basis of empirical studies (Refs. 6.7, 6.9, and 6.11), ACI Code 9.5.2 specifies that *additional* long-term deflections Δ_l due to the combined effects of creep and shrinkage shall be calculated by multiplying the immediate deflection Δ_i by the factor

$$\cdot = \frac{\cdot}{1 + 50 \cdot \cdot} \tag{6.11}$$

where $\cdot' = A_s' \cdot bd$ and $\cdot$ is a time-dependent coefficient that varies as shown in Fig. 6.8. In Eq. (6.11), the quantity $1 \cdot (1 + 50 \cdot ')$ is a reduction factor that is essentially a section property, reflecting the beneficial effect of compression reinforcement A_s' in reducing long-term deflections, whereas $\cdot$ is a material property depending on creep and shrinkage characteristics. For simple and continuous spans, the value of $\cdot'$ used in Eq. (6.11) should be that at the midspan section, according to the ACI Code, or that at the support for cantilevers. Equation (6.11) and the values of $\cdot$ given by Fig. 6.8 apply to

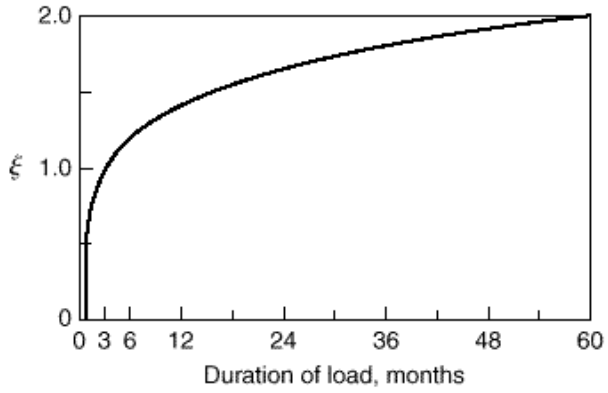

FIGURE 6.8
Time variation of · for long-term deflections.

both normal-weight and lightweight concrete beams. The additional, time-dependent deflections are thus found using values of · from Eq. (6.11) in Eq. (6.6).

Values of · given in the ACI Code and Commentary are satisfactory for ordinary beams and one-way slabs, but may result in underestimation of time-dependent deflections of two-way slabs, for which Branson has suggested a five-year value of · = 3.0 (Ref. 6.7).

Research by Paulson, Nilson, and Hover indicates that Eq. (6.11) does not properly reflect the reduced creep that is characteristic of higher-strength concretes (Ref. 6.14). As indicated in Table 2.1, the creep coefficient for high-strength concrete may be as low as one-half the value for normal concrete. Clearly, the long-term deflection of high-strength concrete beams under sustained load, expressed as a ratio of immediate elastic deflection, correspondingly will be less. This suggests a lower value of the material modifier · in Eq. (6.11) and Fig. 6.8. On the other hand, in high-strength concrete beams, the influence of compression steel in reducing creep deflections is less pronounced, requiring an adjustment in the section modifier 1·(1 + 50· ′) in that equation.

Based on long-term tests involving six experimental programs, the following modified form of Eq. (6.11) is recommended (Ref. 6.14):

$$\cdot = \frac{\cdot\ \cdot}{1 + 50 \cdot \cdot\ \cdot} \tag{6.12}$$

in which

$$\cdot = 1.4 - f_{\dot{c}} \cdot 10{,}000$$

$$0.4 \leq \cdot \leq 1.0 \tag{6.13}$$

The proposed equation gives results identical to Eq. (6.11) for concrete strengths of 4000 psi and below, and much improved predictions for concrete strengths between 4000 and 12,000 psi.

e. Permissible Deflections

To ensure satisfactory performance in service, ACI Code 9.5.2 imposes certain limits on deflections calculated according to the procedures just described. These limits are

TABLE 6.2
Maximum allowable computed deflections

Type of Member	Deflection to Be Considered	Deflection Limitation
Flat roofs not supporting or attached to nonstructural elements likely to be damaged by large deflections	Immediate deflection due to the live load L	$\frac{l}{180}$
Floors not supporting or attached to nonstructural elements likely to be damaged by large deflections	Immediate deflection due to the live load L	$\frac{l}{360}$
Roof or floor construction supporting or attached to nonstructural elements likely to be damaged by large deflections	That part of the total deflection occurring after attachment of the nonstructural elements (sum of the long-time deflection due to all sustained loads and the immediate deflection due to any additional live load)	$\frac{l}{480}$
Roof or floor construction supporting or attached to nonstructural elements not likely to be damaged by large deflections		$\frac{l}{240}$

given in Table 6.2. Limits depend on whether or not the member supports or is attached to other nonstructural elements, and whether or not those nonstructural elements are likely to be damaged by large deflections. When long-term deflections are computed, that part of the deflection that occurs before attachment of the nonstructural elements may be deducted; information from Fig. 6.8 is useful for this purpose. The last two limits of Table 6.2 may be exceeded under certain conditions, according to the ACI Code.

EXAMPLE 6.2

Deflection calculation. The beam shown in Fig. 6.9 is a part of the floor system of an apartment house and is designed to carry calculated dead load w_d of 1.65 kips/ft and a service live load w_l of 3.3 kips/ft. Of the total live load, 20 percent is sustained in nature, while 80 percent will be applied only intermittently over the life of the structure. Under full dead and live load, the moment diagram is as shown in Fig. 6.9*c*. The beam will support nonstructural partitions that would be damaged if large deflections were to occur. They will be installed shortly after construction shoring is removed and dead loads take effect, but before significant creep occurs. Calculate that part of the total deflection that would adversely affect the partitions, i.e., the sum of long-time deflection due to dead and partial live load plus the immediate deflection due to the nonsustained part of the live load. Material strengths are $f'_c = 4000$ psi and $f_y = 60$ ksi.

SOLUTION. For the specified materials, $E_c = 57{,}000 \cdot \sqrt{4000} = 3.60 \times 10^6$ psi, and with $E_s = 29 \times 10^6$ psi, the modular ratio $n = 8$. The modulus of rupture $f_r = 7.5 \cdot \sqrt{4000} = 474$ psi. The effective moment of inertia will be calculated for the moment diagram shown in Fig. 6.9*c* corresponding to the full service load, on the basis that the extent of cracking will be governed by the full service load, even though that load is intermittent. In the positive-moment region, the centroidal axis of the uncracked T section of Fig. 6.9*b* is found by taking moments about the top surface, to be at 7.66 in. depth, and $I_g = 33{,}160$ in^4. By similar means, the centroidal axis of the cracked transformed T section shown in Fig. 6.9*d* is located

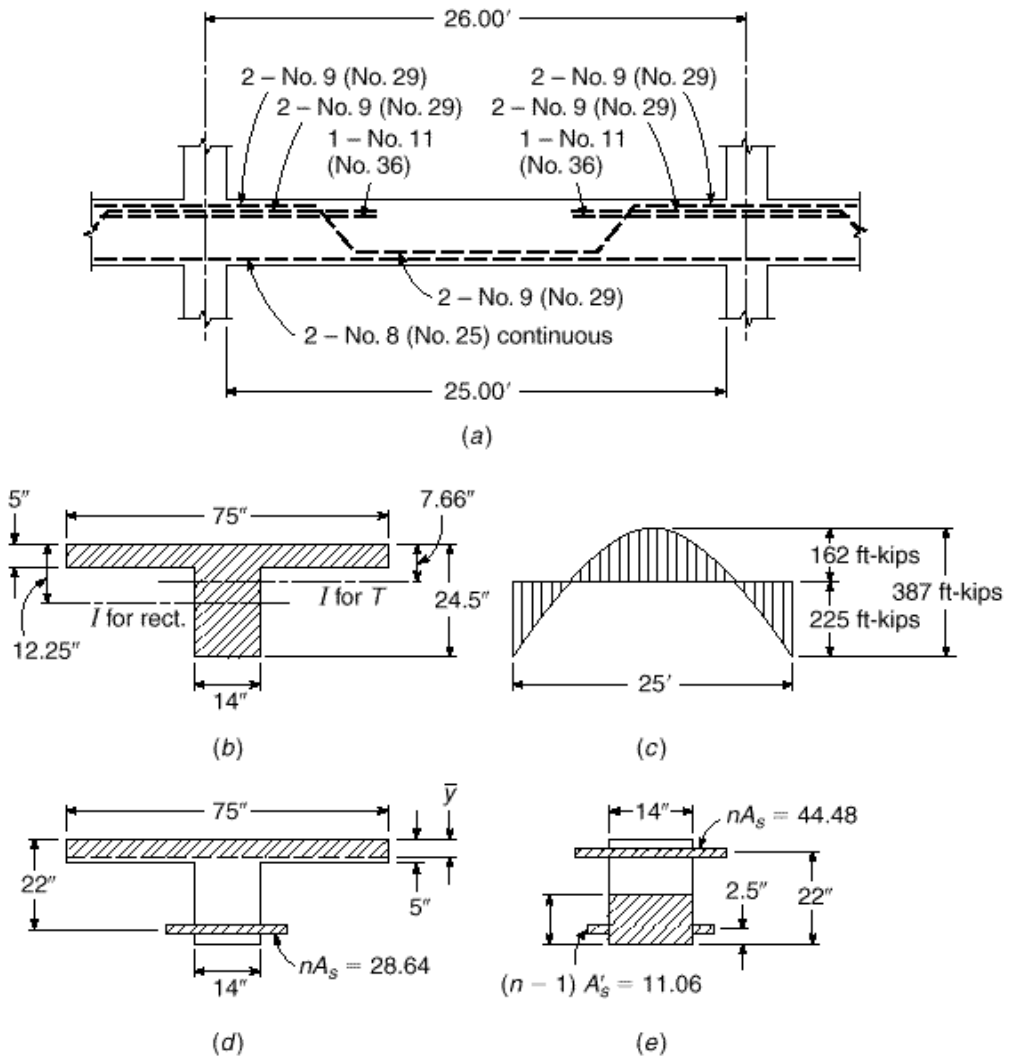

FIGURE 6.9
Continuous T beam for deflection calculations in Example 6.2.

3.73 in. below the top of the slab and $I_{cr} = 10{,}860$ in^4. The cracking moment is then found by means of Eq. (6.7):

$$M_{cr} = 474 \times \frac{33{,}160}{16.84} \times \frac{1}{12{,}000} = 78 \text{ ft-kips}$$

With $M_{cr} \cdot M_a = 78 \cdot 162 = 0.481$, the effective moment of inertia in the positive bending region is found from Eq. (6.8) to be

$$I_e = 0.481^3 \times 31{,}160 + \cdot 1 - 0.481^3 \cdot \times 10{,}860 = 13{,}120 \text{ in}^4$$

In the negative bending region, the gross moment of inertia will be based on the rectangular section shown in Fig. 6.9*b*. For this area, the centroid is 12.25 in. from the top surface and $I_g = 17{,}200$ in^4. For the cracked transformed section shown in Fig. 6.9*e*, the centroidal axis is found, taking moments about the bottom surface, to be 8.65 in. from that level, and $I_{cr} = 11{,}366$ in^4. Then

$$M_{cr} = 474 \times \frac{17{,}200}{12.25} \times \frac{1}{12{,}000} = 55.5 \text{ ft-kips}$$

giving $M_{cr}/M_a = 55.5/225 = 0.247$. Thus, for the negative-moment regions,

$$I_e = 0.247^3 \times 17{,}200 + [1 - 0.247^3] \times 11{,}366 = 11{,}450 \text{ in}^4$$

The average value of I_e to be used in calculation of deflection is

$$I_{e,av} = \frac{1}{2}[13{,}120 + 11{,}450] = 12{,}285 \text{ in}^4$$

It is next necessary to find the sustained-load deflection multiplier given by Eq. (6.11) and Fig. 6.8. For the positive bending zone, with no compression reinforcement, $\lambda_{pos} = 2.00$.

For convenient reference, the deflection of the member under full dead plus live load of 4.95 kips/ft, corresponding to the moment diagram of Fig. 6.9*c*, will be found. Making use of the moment-area principles,

$$\Delta_{d+l} = \frac{1}{EI}\left[\frac{2}{3} \times 387 \times 12.5 \times \frac{5}{8} \times 12.5 - 225 \times 12.5 \times 6.25\right] = \frac{7620}{EI}$$

$$= \frac{7620 \times 1728}{3600 \times 12{,}285} = 0.298 \text{ in.}$$

Using this figure as a basis, the time-dependent portion of dead load deflection (the only part of the total that would affect the partitions) is

$$\Delta_d = 0.298 \times \frac{1.65}{4.95} \times 2.00 = 0.199 \text{ in.}$$

while the sum of the immediate and time-dependent deflection due to the sustained portion of the live load is

$$\Delta_{0.20l} = 0.298 \times \frac{3.3}{4.95} \times 0.20 \times 3.00 = 0.119 \text{ in.}$$

and the instantaneous deflection due to application of the short-term portion of the live load is

$$\Delta_{0.80l} = 0.298 \times \frac{3.3}{4.95} \times 0.80 = 0.159 \text{ in.}$$

Thus the total deflection that would adversely affect the partitions, from the time they are installed until all long-time and subsequent instantaneous deflections have occurred, is

$$\Delta = 0.199 + 0.119 + 0.159 = 0.477 \text{ in.}$$

For comparison, the limitation imposed by the ACI Code in such circumstances is $l/480 = 26 \times 12/480 = 0.650$ in., indicating that the stiffness of the proposed member is sufficient.

It may be noted that relatively little error would have been introduced in the above solution if the cracked-section moment of inertia had been used for both positive and negative sections rather than I_e. Significant savings in computational effort would have resulted. If M_{cr}/M_a is less than $\frac{1}{3}$, use of I_{cr} would almost always be acceptable. It should be noted further that computation of the moment of inertia for both uncracked and cracked sections is greatly facilitated by design aids like those included in Ref. 6.15.

6.8 Deflections Due to Shrinkage and Temperature Changes

Concrete shrinkage will produce compressive stress in the longitudinal reinforcement in beams and slabs and equilibrating tensile stress in the concrete. If, as usual, the reinforcement is not symmetrically placed with respect to the concrete centroid, then

shrinkage will produce curvature and corresponding deflection. The deflections will be in the same direction as those produced by the loads, if the reinforcement is mainly on the side of the member subject to flexural tension.

Shrinkage deflection is not usually calculated separately, but is combined with creep deflection, according to ACI Code procedures (see Section 6.7d). However, there are circumstances where a separate and more accurate estimation of shrinkage deflection may be necessary, particularly for thin, lightly loaded slabs. Compression steel, while it has only a small effect in reducing immediate elastic deflections, contributes significantly in reducing deflections due to shrinkage (as well as creep), and is sometimes added for this reason.

Curvatures due to shrinkage of concrete in an unsymmetrically reinforced concrete member can be found by the fictitious tensile force method (Ref. 6.7). Figure 6.10*a* shows the member cross section, with compression steel area A_s' and tensile steel area A_s, at depths d' and d, respectively, from the top surface. In Fig. 6.10*b*, the concrete and steel are imagined to be temporarily separated, so that the concrete can assume its free shrinkage strain ϵ_{sh}. Then a fictitious compressive force $T_{sh} = \epsilon_{sh} A_s + A_s \epsilon_{sh} E_s$ is applied to the steel, at the centroid of all the bars, a distance e below the concrete centroid, such that the steel shortening will exactly equal the free shrinkage strain of the concrete. The equilibrating tension force T_{sh} is then applied to the recombined section, as in Fig. 6.10*c*. This produces a moment $T_{sh}e$, and the corresponding shrinkage curvature is

$$\phi_{sh} = \frac{T_{sh} e}{EI}$$

The effects of concrete cracking and creep complicate the analysis, but comparisons with experimental data (Ref. 6.7) indicate that good results can be obtained using e_g and I_g for the uncracked gross concrete section and by using a reduced modulus E_{cf} equal to $\frac{1}{2} E_c$ to account for creep. Thus

$$\phi_{sh} = \frac{2 T_{sh} e_g}{E_c I_g} \tag{6.14}$$

where E_c is the usual value of concrete modulus given by Eq. (2.3).

Empirical methods are also used, in place of the fictitious tensile force method, to calculate shrinkage curvatures. These methods are based on the simple but reasonable proposition that the shrinkage curvature is a direct function of the free shrinkage and steel percentage, and an inverse function of the section depth (Ref. 6.7). Branson

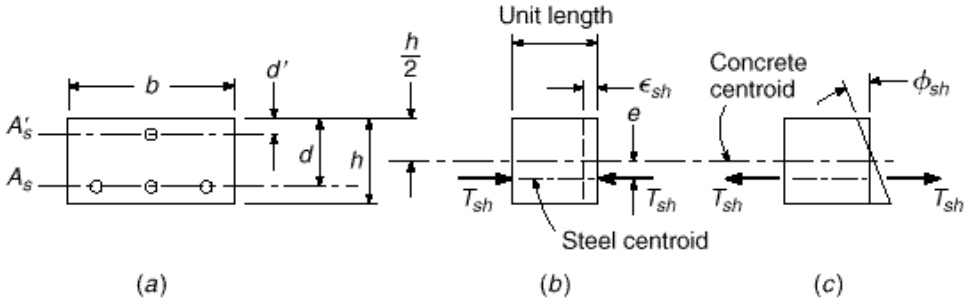

FIGURE 6.10
Shrinkage curvature of a reinforced concrete beam or slab: (*a*) cross section; (*b*) free shrinkage strain; (*c*) shrinkage curvature.

suggests that for steel percentage $(p - p') \leq 3$ percent (where $p = 100A_s/bd$ and $p' = 100A'_s/bd$),

$$\phi_{sh} = 0.7\frac{\varepsilon_{sh}}{h}\sqrt{p - p'}\left(1.3 - \frac{p - p'}{p}\right)^{1.2} \tag{6.15a}$$

and for $(p - p') > 3$ percent,

$$\phi_{sh} = \frac{\varepsilon_{sh}}{h} \tag{6.15b}$$

With shrinkage curvature calculated by either method, the corresponding member deflection can be determined by any convenient means such as the moment-area or conjugate-beam method. If steel percentages and eccentricities are constant along the span, the deflection Δ_{sh} resulting from the shrinkage curvature can be determined from

$$\Delta_{sh} = K_{sh}\phi_{sh}l^2 \tag{6.16}$$

where K_{sh} is a coefficient equal to 0.500 for cantilevers, 0.125 for simple spans, 0.065 for interior spans of continuous beams, and 0.090 for end spans of continuous beams (Ref. 6.7).

EXAMPLE 6.3

Shrinkage deflection. Calculate the midspan deflection of a simply supported beam of 20 ft span due to shrinkage of the concrete for which $\varepsilon_{sh} = 780 \times 10^{-6}$. With reference to Fig. 6.10*a*, $b = 10$ in., $d = 17.5$ in., $h = 20$ in., $A_s = 3.00$ in^2, and $A'_s = 0$. The elastic moduli are $E_c = 3.6 \times 10^6$ psi and $E_s = 29 \times 10^6$ psi.

SOLUTION. By the fictitious tensile force method,

$$T_{sh} = 3.00 \times 780 \times 10^{-6} \times 29 \times 10^6 = 67{,}900 \text{ lb}$$

and from Eq. (6.14) with $I_g = 6670$,

$$\phi_{sh} = \frac{2 \times 67{,}900 \times 7.5}{3.6 \times 10^6 \times 6670} = 42.4 \times 10^{-6}$$

while from Eq. (6.16) with $K_{sh} = 0.125$ for the simple span,

$$\Delta_{sh} = 0.125 \times 42.4 \times 10^{-6} \times 240^2 = 0.305 \text{ in.}$$

Alternatively, by Branson's approximate Eq. (6.15*a*) with $p = 100 \times 3.175 = 1.7$ percent and $p' = 0$,

$$\Delta_{sh} = \frac{0.7 \times 780 \times 10^{-6}}{20}\sqrt{1.7}(1.3)^{1.2} = 32.5 \times 10^{-6}$$

compared with 42.4×10^{-6} obtained by the equivalent tensile force method. Considering the uncertainties such as the effects of cracking and creep, the approximate approach can usually be considered satisfactory.

Deflections will be produced as a result of differential temperatures varying from top to bottom of a member also. Such variation will result in a strain variation with member depth that may usually be assumed to be linear. For such cases, the deflection due to differential temperature can be calculated using Eq. (6.16) in which ϕ_{sh} is replaced by $\alpha\Delta T/h$, where the thermal coefficient α for concrete may be taken as 5.5×10^{-6} per °F and ΔT is the temperature differential in degrees Fahrenheit from

one side to the other. The presence of the reinforcement has little influence on curvatures and deflections resulting from differential temperatures, because the thermal coefficient for the steel (6.5×10^{-6}) is very close to that for concrete.

6.9 Moment vs. Curvature for Reinforced Concrete Sections

Although it is not needed explicitly in ordinary design and is not a part of ACI Code procedures, the relation between moment applied to a given beam section and the resulting curvature, through the full range of loading to failure, is important in several contexts. It is basic to the study of member ductility, understanding the development of plastic hinges, and accounting for the redistribution of elastic moments that occurs in most reinforced concrete structures before collapse (see Section 12.9).

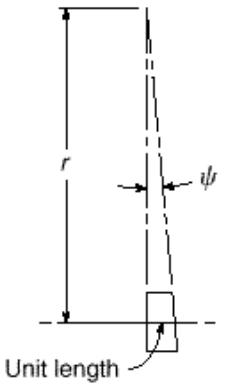

FIGURE 6.11
Unit curvature resulting from bending of beam section.

It will be recalled, with reference to Fig. 6.11, that curvature is defined as the angle change per unit length at any given location along the axis of a member subjected to bending loads:

$$\phi = \frac{1}{r} \tag{6.17}$$

where ϕ = unit curvature and r = radius of curvature. With the stress-strain relationships for steel and concrete, represented in idealized form in Fig. 6.12*a* and *b*, respectively, and the usual assumptions regarding perfect bond and plane sections, it is possible to calculate the relation between moment and curvature for a typical underreinforced concrete beam section, subject to flexural cracking, as follows.

Figure 6.13*a* shows the transformed cross section of a rectangular, tensile-reinforced beam in the uncracked elastic stage of loading, with steel represented by the equivalent concrete area nA_s, i.e., with area $(n-1)A_s$ added outside of the rectangular concrete section.† The neutral axis, a distance c_1 below the top surface of the beam, is easily found (see Section 3.3a). In the limiting case, the concrete stress at the tension face is just equal to the modulus of rupture f_r and the strain is $\varepsilon_r = f_r/E_c$. The steel is well below yield at this stage, which can be confirmed by computing, from the strain diagram, the steel strain $\varepsilon_s = \varepsilon_{cs}$, where ε_{cs} is the concrete strain at the level of the steel. It is easily confirmed, also, that the maximum concrete compressive stress will be well below the proportional limit. The curvature is seen, in Fig. 6.13*b*, to be

$$\phi_{cr} = \frac{\varepsilon_1}{c_1} = \frac{\varepsilon_r}{c_2} \tag{6.18}$$

and the corresponding moment is

$$M_{cr} = \frac{f_r I_{ut}}{c_2} \tag{6.19}$$

where I_{ut} is the moment of inertia of the uncracked transformed section. Equations (6.18) and (6.19) provide the information needed to plot point 1 of the moment-curvature graph of Fig. 6.16*a*.

† Note that compression reinforcement, or multiple layers of tension reinforcement, can easily be included in the analysis with no essential complication.

FIGURE 6.12
Idealized stress-strain curves: (*a*) steel; (*b*) concrete.

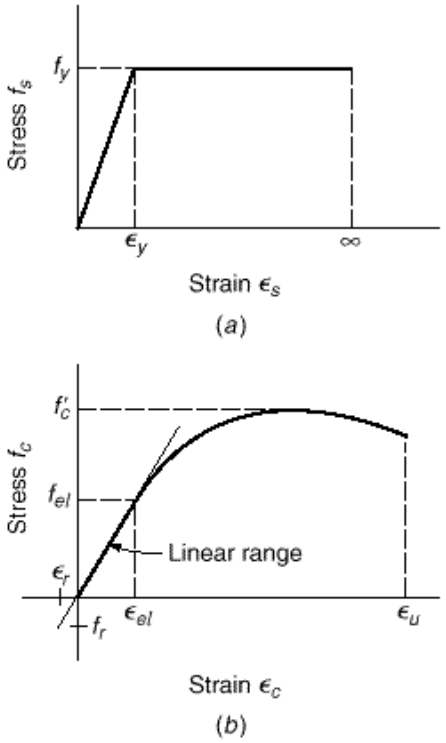

FIGURE 6.13
Uncracked beam in the elastic range of loading: (*a*) transformed cross section; (*b*) strains; (*c*) stresses and forces.

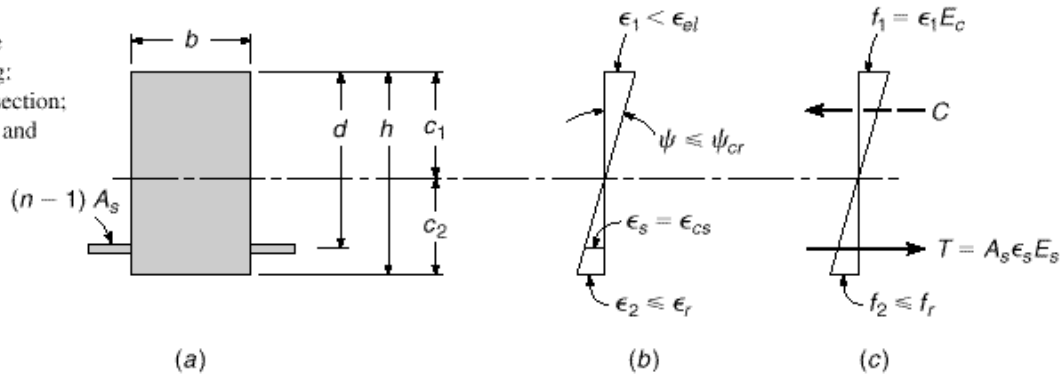

When tensile cracking occurs at the section, the stiffness is immediately reduced, and curvature increases to point 2 in Fig. 6.16 with no increase in moment. The analysis now is based on the cracked transformed section of Fig. 6.14*a*, with steel represented by the transformed area nA_s and tension concrete deleted. The cracked, elastic neutral axis distance $c_1 = kd$ is easily found by the usual methods (see Section 3.3b). In the limiting case, the concrete strain just reaches the proportional limit, as shown in Fig. 6.14*b*, and, typically, the steel is still below the yield strain. The curvature is easily computed by

$$\cdot_{el} = \frac{\cdot_1}{c_1} = \frac{\cdot_{el}}{c_1} \tag{6.20}$$

FIGURE 6.14
Cracked beam in the elastic range of material response: (*a*) transformed cross section; (*b*) strains; (*c*) stresses and forces.

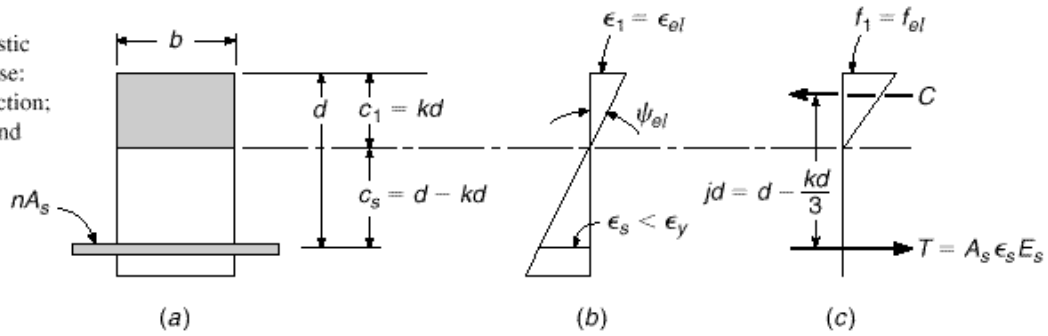

and the corresponding moment is

$$M_{el} = \frac{1}{2} f_{el} kjbd^2 \tag{6.21}$$

as was derived in Section 3.3b. This provides point 3 in Fig. 6.16. The curvature at point 2 can now be found from the ratio $M_{cr} \cdot M_{el}$.

Next, the cracked, inelastic stage of loading is shown in Fig. 6.15. Here the concrete is well into the inelastic range, although the steel has not yet yielded. The neutral axis depth c_1 is less than the elastic kd and is changing with increasing load as the shape of the concrete stress distribution changes and the steel stress changes.

It is now convenient to adopt a numerical representation of the concrete compressive stress distribution, to find both the total concrete compressive force C and the location of its centroid, for any arbitrarily selected value of maximum concrete strain $\cdot_1$ in this range. The compressive strain diagram is divided into an arbitrary number of steps (e.g., four, in Fig. 6.15*b*), and the corresponding compressive stresses for each strain read from the stress-strain curve of Fig. 6.12*b*. The stepwise representation of the actual continuous stress block is integrated numerically to find C, and its point of application is located, taking moments of the concrete forces about the top of the section. The basic equilibrium requirement, $C = T$, then can be used to find the correct location of the neutral axis, for the particular compressive strain selected, following an iterative procedure.

FIGURE 6.15
Cracked beam with concrete in the inelastic range of loading: (*a*) cross section; (*b*) strains; (*c*) stresses and forces.

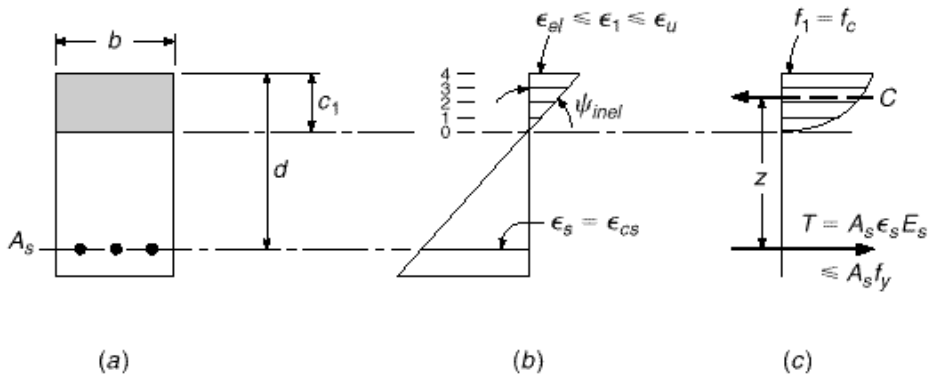

The entire process can be summarized as follows:

1. Select any top face concrete strain ε_1 in the inelastic range, i.e., between ε_{el} and ε_u.
2. Assume the neutral axis depth, a distance c_1 below the top face.
3. From the strain diagram geometry, determine $\varepsilon_s = \varepsilon_{cs}$.
4. Compute $f_s = \varepsilon_s E_s$, but $\leq f_y$, and $T = A_s f_s$.
5. Determine C by integrating numerically under the concrete stress distribution curve.
6. Check to see if $C = T$. If not, the neutral axis must be adjusted upward or downward, for the particular concrete strain that was selected in step 1, until equilibrium is satisfied. This determines the correct value of c_1.

Curvature can then be found from

$$\psi_{inel} = \frac{\varepsilon_1}{c_1} \tag{6.22}$$

The internal lever arm z from the centroid of the concrete stress distribution to the tensile resultant, Fig. 6.15*c*, is calculated, after which

$$M_{inel} = Cz = Tz \tag{6.23}$$

The sequence of steps 1 through 6 is then repeated for newly selected values of concrete strain ε_1. The end result will be a series of points, such as 4, 5, 6, and 7 in Fig. 6.16. The limit of the moment-curvature plot is reached when the concrete top face strain equals ε_u, corresponding to point 7. The steel would be well past the yield strain at this loading, and at the yield stress.

It is important to be aware of the difference between a moment-unit curvature plot, such as Fig. 6.16, and a moment-rotation diagram for the hinging region of a reinforced concrete beam. The hinging region normally includes a number of discrete cracks, but between those cracks, the uncracked concrete reduces the steel strain, leading to what is termed the *tension stiffening* effect. The result is that the total rotation at the hinge is much less than would be calculated by multiplying the curvature per

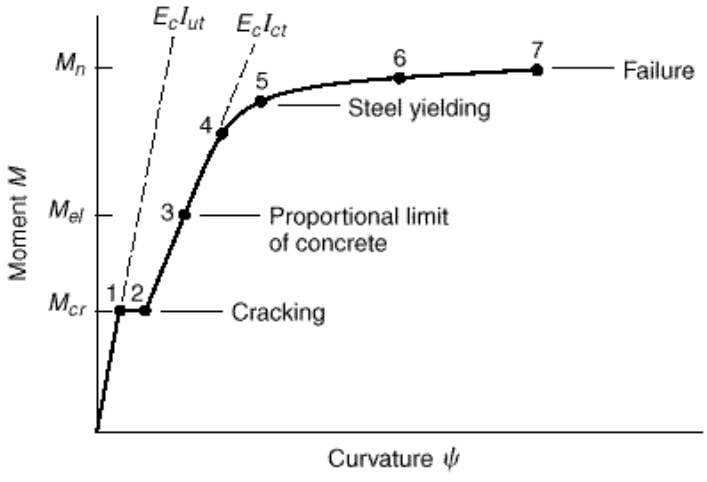

FIGURE 6.16
Moment-curvature relation for tensile-reinforced beam.

unit length at the cracked section by the observed or assumed length of the hinging region. Furthermore, the sharp increase in unit curvature shown in Fig. 6.16 at cracking would not be seen on the moment-rotation plot, only a small, but progressive, reduction of the slope of the diagram.

REFERENCES

6.1. ACI Committee 224, "Control of Cracking in Concrete Structures (ACI 224R-01)," *ACI Manual of Concrete Practice*, Part 2, American Concrete Institute, Farmington Hills, MI, 2003.

6.2. P. Gergely and L. A. Lutz, "Maximum Crack Width in Reinforced Concrete Flexural Members," in *Causes, Mechanisms, and Control of Cracking in Concrete*, SP-20, American Concrete Institute, Detroit, MI, 1968, pp. 1–17.

6.3. P. H. Kaar and A. H. Mattock, "High-Strength Bars as Concrete Reinforcement—Part 4: Control of Cracking," *Journal*, PCA Research and Development Laboratories, vol. 5, no. 1, 1963, pp. 15–38.

6.4. R. J. Frosch, "Another Look at Cracking and Crack Control in Reinforced Concrete," *ACI Struct. J.*, vol. 96, no. 3, 1999, pp. 437–442.

6.5. B. B. Broms, "Crack Width and Crack Spacing in Reinforced Concrete Members," *J. ACI*, vol. 62, no. 10, 1965, pp. 1237–1256.

6.6. ACI Committee 318, "Discussion of Proposed Revisions to Building Code Requirements for Structural Concrete (ACI 318-95) and Commentary (ACI 318R-95)," *Concr. Intl.*, vol. 21, no. 5, 1999, pp. 318-1–318-49.

6.7. D. E. Branson, *Deformation of Concrete Structures*, McGraw-Hill, New York, 1977.

6.8. ACI Committee 435, "Control of Deflection in Concrete Structures (ACI 435R-95)," *ACI Manual of Concrete Practice*, Part 5, American Concrete Institute, Farmington Hills, MI, 2003.

6.9. W. W. Yu and G. Winter, "Instantaneous and Long-Time Deflections of Reinforced Concrete Beams Under Working Loads," *J. ACI*, vol. 57, no. 1, 1960, pp. 29–50.

6.10. ACI Committee 209, "Prediction of Creep, Shrinkage and Temperature Effects in Concrete Structures (ACI 209R-92)," *ACI Manual of Concrete Practice*, Part 1, 2003.

6.11. D. E. Branson, "Compression Steel Effect on Long-Time Deflections," *J. ACI*, vol. 68, no. 8, 1971, pp. 555–559.

6.12. ACI Committee 435, "Proposed Revisions by Committee 435 to ACI Building Code and Commentary Provisions on Deflections," *J. ACI*, vol. 75, no. 6, June 1978, pp. 229–238.

6.13. C. H. Norris, J. B. Wilbur, and S. Utku, *Elementary Structural Analysis*, 4th ed., McGraw-Hill, New York, 1991.

6.14. K. Paulson, A. H. Nilson, and K. C. Hover, "Long-Term Deflection of High-Strength Concrete Beams," *ACI Materials Journal*, vol. 88, no. 2, 1991, pp. 197–206.

6.15. *CRSI Handbook*, 9th ed., Concrete Reinforcing Steel Institute, Schaumburg, IL, 2002.

PROBLEMS

6.1. A rectangular beam of width $b = 12$ in., effective depth $d = 20.5$ in., and total depth $h = 23$ in. spans 18.5 ft between simple supports. It will carry a computed dead load of 1.27 kips/ft including self-weight, plus a service live load of 2.69 kips/ft. Reinforcement consists of four evenly spaced No. 8 (No. 25) bars in one row. The clear cover on the sides is 2 in. Material strengths are $f_y = 60{,}000$ psi and $f'_c = 4000$ psi.

(*a*) Compute the stress in the steel at full service load, and using the Gergely-Lutz equation estimate the maximum crack width.

(*b*) Confirm the suitability of the proposed design based on Fig. (6.3).

6.2. To save steel-handling costs, an alternative design is proposed for the beam in Problem 6.1, using two No. 10 (No. 32) Grade 75 bars to provide approximately the same steel strength as the originally proposed four No. 8 (No. 25) Grade 60 bars. Check to determine if the redesigned beam is satisfactory with respect to cracking according to the ACI Code. What modification could you

suggest that would minimize the number of bars to reduce cost, yet satisfy requirements of crack control?

6.3. For the beam in Problem 6.1:

(*a*) Calculate the increment of deflection resulting from the first application of the short-term live load.

(*b*) Find the creep portion of the sustained load deflection plus the immediate deflection due to live load.

(*c*) Compare your results with the limitations imposed by the ACI Code, as summarized in Table 6.2.

Assume that the beam is a part of a floor system and supports cinder block partitions susceptible to cracking if deflections are excessive.

6.4. A beam having $b = 12$ in., $d = 21.5$ in., and $h = 24$ in. is reinforced with three No. 11 (No. 36) bars. Material strengths are $f_y = 60{,}000$ psi and $f'_c = 4000$ psi. It is used on a 28 ft simple span to carry a total service load of 2430 lb/ft. For this member, the sustained loads include self-weight of the beam plus additional superimposed dead load of 510 lb/ft, plus 400 lb/ft representing that part of the live load that acts more or less continuously, such as furniture, equipment, and time-average occupancy load. The remaining 1220 lb/ft live load consists of short-duration loads, such as the brief peak load in the corridors of an office building at the end of a working day.

(*a*) Find the increment of deflection under sustained loads due to creep.

(*b*) Find the additional deflection increment due to the intermittent part of the live load.

In your calculations, you may assume that the peak load is applied almost immediately after the building is placed in service, then reapplied intermittently. Compare with ACI Code limits from Table 6.2. Assume that, for this long-span floor beam, construction details are provided that will avoid damage to supported elements due to deflections. If ACI Code limitations are not met, what changes would you recommend to improve the design?

6.5. A reinforced concrete beam is continuous over two equal 22 ft spans, simply supported at the two exterior supports, and fully continuous at the interior support. Concrete cross-section dimensions are $b = 10$ in., $h = 22$ in., and $d = 19.5$ in. for both positive and negative bending regions. Positive reinforcement in each span consists of two No. 9 (No. 29) bars, and negative reinforcement at the interior support is made up of three No. 10 (No. 32) bars. No compression steel is used. Material strengths are $f_y = 60{,}000$ psi and $f'_c = 5000$ psi. The beam will carry a service live load, applied early in the life of the member, of 1800 lb/ft distributed uniformly over both spans; 20 percent of this load will be sustained more or less permanently, while the rest is intermittent. The total service dead load is 1000 lb/ft including self-weight.

(*a*) Find the immediate deflection when shores are removed and the full dead load is applied.

(*b*) Find the long-term deflection under sustained load.

(*c*) Find the increment of deflection when the short-term part of the live load is applied.

Compare with ACI Code deflection limits; piping and brittle conduits are carried that would be damaged by large deflections. Note that midspan deflection may be used as a close approximation of maximum deflection.

6.6. Recalculate the deflections of Problem 6.5 based on the assumption that 20 percent of the live load represents the normal service condition of loading and

is sustained more or less continuously, while the remaining 80 percent is a short-term peak loading that would probably not be applied until most creep deflections have occurred. Compare with your earlier results.

6.7. The tensile-reinforced rectangular beam shown in Fig. P6.7 is made using steel with $f_y = 60{,}000$ psi and $E_s = 29{,}000{,}000$ psi. A perfectly plastic response after yielding can be assumed. The concrete has a stress-strain curve in compression that may be approximated by the parabola $f_c = f'_c[2\varepsilon_c/\varepsilon_0 - (\varepsilon_c/\varepsilon_0)^2]$, where f_c and ε_c are the stress and strain in the concrete. The variable ε_0 is the strain at the peak stress = 0.002, and $f'_c = 4000$ psi. The ultimate strain in the concrete is 0.003. The concrete responds elastically in tension up to the modulus of rupture $f_r = 475$ psi. Based on this information, plot a curve relating applied moment to unit curvature at a section subjected to flexural cracking. Label points corresponding to first cracking, first yielding of steel, and peak moment.

FIGURE P6.7